THE ANALYSIS OF CYCLOGYRO USING UNSTEADY VORTEX LATTICE METHOD

Hu Yu, Tay Wee Beng, Lim Kah Bin
*** Department of Mechanical Engineering, 9 Engineering Drive 1, National University of Singapore, Singapore, 117576**

Keywords: *Cyclogyro,Cycloidal propeller, Unsteady Vortex Lattice method, MAV*

Abstract

The investigation on analysis of a cyclogyro using Unsteady Vortex Lattice Method (UVLM) is presented in this paper. There exists many simplified method for cyclogyro design analysis, but they are quite crude and do not fully deal with problems with complex configurations and motion patterns. By solving N-S equations using the CFD algorithms can solve the problem but the cost is too high. The UVLM is a good choice in this case since it can solve very complex configuration with complicated wing motion pattern. It only needs to generate grids on wing surfaces and wake. So UVLM is selected for the design simulation of cyclogyro in this paper. The comparison was made between the UVLM and the experiment data. The comparison indicates that UVLM can provide good results for cycloidal propellers and can be applied in the design analysis of cyclogyroes.

1 Introduction

The cyclogyro is a type of airplane equipped with cycloidal propellers. The cycloidal propeller is composed of two to more blades that rotates around an axis parallel to the blades. When the aircraft hovers, the blades travels along a circle and when the aircraft moves backward or forward, the blades travels along a cycloid. The pitch angles of the blades are controlled by an eccentric mechanism. By setting the offset of the eccentric, the desired amplitude of the aerodynamic forces (i.e., Lift or Thrust) can be obtained. By varying the phase angle of the eccentric, the direction of the total force vector can be varied from 0 to 360 deg. This property provides the aircraft with 360deg vector trusting, which greatly improves the maneuverability of the airplane.

Our effort is to develop a MAV using the concept of cyclogyro. But the design of an aircraft needs comparison among vast varieties of designs. Therefore large amounts of simulation are required. Unfortunately, the motion of the blades on cycloidal propeller is quite complex and unsteady; therefore the design simulation of the cyclogyro will be a challenging task. The algorithm for design simulation should be both accurate and less time consuming.

There exist many algorithms for cycloidal propellers. But these algorithms are too rough to be adopted when we want to study the details of the design. Another choice is to solve the N-S function using the CFD algorithms and deploy grids in the flow field. Undoubtedly, they are too expensive.

So we turned to the Unsteady Vortex Lattice method (UVLM). The UVLM only requires the grids to be generated on the body surfaces and wake sheet, therefore it will be less time consuming than other CFD algorithms [1, 2]. The UVLM can also take the effects of wakes and the inference of all blades into account and simulate the blades with very complex configuration and motion pattern.

2 . The Unsteady Vortex Lattice Method

The unsteady vortex lattice method (UVLM) is based on the potential theory which assumes non-viscous and irritation flow. Since the unsteady vortex panel method can deal with the blade wake, the inference of the blades, very

complex wing shapes and motion pattern, it enables one to get better understand on the aerodynamics of the cyclogyroes.

2.1 The potential flow model

For the ir-rotational flow, the vorticity is zero and the velocity potential can be defined:

$$\nabla\Phi = \vec{q} \quad (1)$$

Substitute Eq 1. into the continuity equation, we can obtain the Laplace's equation:

$$\nabla^2\Phi = 0 \quad (2)$$

The Laplace's equation will be solved with boundary conditions about the body surface S_B, wake surface S_w and outer boundary S_∞. With the Green's identity, the equation for the velocity potential at any point in the flow field p can be obtained [1].

$$\Phi(p)=\frac{1}{4\pi}\int_{S_B}\left[\frac{1}{r}\nabla(\Phi-\Phi_i)-(\Phi-\Phi_i)\nabla\frac{1}{r}\right]\cdot\vec{n}dS-\frac{1}{4\pi}\int_{S_w}\left(\Phi\vec{n}\cdot\nabla\frac{1}{r}\right)dS+\Phi_\infty \quad (3)$$

Where r is the distance between point p and the singularity on the boundary surface. $\vec{n}$ is the normal unit vector on the boundaries and points outside the regions of interest.

If we define $-\mu = \Phi - \Phi_i$ and $-\sigma = \frac{\partial\Phi}{\partial n} - \frac{\partial\Phi_i}{\partial n}$, then we have:

$$\Phi(p) = -\frac{1}{4\pi}\int_{S_B}\left[\frac{1}{r}\sigma-\mu\nabla\frac{1}{r}\right]dS+\frac{1}{4\pi}\int_{S_w}\left(\mu\vec{n}\cdot\nabla\frac{1}{r}\right)dS+\Phi_\infty \quad (4)$$

From equation 4, we can obtain the velocity potential at point P with distribution of doublet strength and source strength on the boundaries. Therefore the problem became to determine doublet strength and source strength on the boundaries.

2.2 The discretization and computation of aerodynamics loads

If discrete the body surface and wake into finite number of panels and apply the boundary condition (either Neumann boundary condition or Dirichlet boundary condition) on the body surface and lift body trailing edge Kutta condition, we can obtain a set of linear equations about the doublet and source strength distribution. If set the source strength $\sigma = \vec{n}\vec{q}_\infty$, then the equations reduced to a set of equations about unknown doublet distribution. By solving this set of equations, the doublet strength can be obtained. Once the strength of the singularities is known, the aerodynamics forces can be obtained by Bernoulli's functions.

For unsteady vortex lattice method, the thickness of the wings is zero, the vortex rings, which are equivalent to the constant strength doublet panels, are deployed on the wing surfaces and the wake sheets. The time marching methodology is applied to formulate the unsteady effects. At the first time step, there are no wake vortex rings and only wing bound vortex exists. The trailing segment of the trailing edge vortex ring represents the starting vortex. Since the Kelvin condition is automatically fulfilled by vortex ring model, we need not add an additional equation. During each time step that follows, the wing will move along its flight path and each trailing edge vortex panel sheds a wake panel with vortex strength equal to its circulation in the previous time step.

In each time step, a set of linear equations about the circulation of the wing bound vortex rings will be obtained by applying Neumann boundary condition at each vortex panel collocation point (Eq.5).

$$\begin{bmatrix} a_{11} & a_{12} & a_{13} & \dots & a_{1n} \\ a_{21} & a_{22} & a_{23} & \dots & a_{31} \\ a_{31} & a_{32} & a_{33} & \dots & a_{3n} \\ & \dots & & \dots & \\ a_{n1} & a_{n2} & a_{n3} & \dots & a_{nn} \end{bmatrix} \begin{pmatrix} \Gamma_1 \\ \Gamma_2 \\ \Gamma_3 \\ \dots \\ \Gamma_n \end{pmatrix} = \begin{pmatrix} RHS_1 \\ RHS_2 \\ RHS_3 \\ \dots \\ RHS_n \end{pmatrix} \quad (5)$$

$$RHS_i = -(U(t)+u_w, V(t)+v_w, W(t)+w_w)\cdot\vec{n}$$

In Eq.5, $a_{i,j}$ is the normal velocity at collocation point i induced by vortex panel j when Γ_j, the circulation of the vortex panel j equals 1. $\sum_{j=1,n} a_{i,j}\Gamma_j$ is the velocity induced by all panels at collocation point i. The term $-RHS_i$ denotes the normal velocity caused by kinematics motion and the velocity wake panels, where $[U(t), V(t), W(t)]$ is the velocity caused by kinetic motion and $[u_w, v_w, w_w]$ is the

velocity caused by wake panels. $\sum_{j=1,n} a_{i,j}\Gamma_j + RHS_i = 0$ means the normal velocity at collocation point i caused by wing bound vortex rings, wake vortex rings and wing motion equals 0, as stated in Neumann boundary condition.

In order to model arbitrary wing motion and simplify the calculation of the velocity cause by kinetic motion. $[U(t), V(t), W(t)]$ is calculated using central difference scheme (CDS) on the position the collocation point.

$$\begin{pmatrix} U(t) \\ V(t) \\ W(t) \end{pmatrix} = \begin{pmatrix} \dfrac{X(t+1)-X(t-1)}{2\cdot dt} \\ \dfrac{Y(t+1)-Y(t-1)}{2\cdot dt} \\ \dfrac{Z(t+1)-Z(t-1)}{2\cdot dt} \end{pmatrix} \quad (6)$$

Where $(X(t), Y(t), Z(t))$ is the position of the collocation point at time step t, and dt is the time step length. With this method, we only need to provide the position of the wings at each step without specifying the wing motion velocities and the computation process can be simplified.

2.3 The aerodynamics forces calculation

As the circulations of the vortex rings are known, we can obtain the pressure distribution by Bernoulli's function [1]:

$$\Delta p = \rho\left[\left(\frac{Q_t^2}{2}\right)_u - \left(\frac{Q_t^2}{2}\right)_l + \left(\frac{\partial\Phi}{\partial t}\right)_u - \left(\frac{\partial\Phi}{\partial t}\right)_l\right] \quad (7)$$

And the aerodynamics forces can be obtained by summing up the pressure distribution:

$$F = \sum_{i=1,n} -(\Delta p_i \Delta S_i)\vec{n} \quad (8)$$

The moment caused by the aerodynamics force can be calculated by summing the moment on each panel $\vec{m}_i$.

$$\vec{M} = \sum_{i=1,n} \vec{m}_i \quad (9)$$

$$\vec{m}_i = \vec{r} \times \vec{F}_i \quad (10)$$

Where $\vec{r}$ is the vector from the origin of the body frame to the location of $\vec{F}_i$, which is the centre of the leading segment of the vortex ring.

2.4 The wake rolling up

Since the wake is force free and carries no loads, the wake panels will move with local free stream. The velocities of the wake vortex ring corners are obtained by evaluate the influence of wing bound vortex rings and wake vortex rings.

2.5 Vortex blob modifications

The Biot-Savart's Law used to evaluate the induced velocity at a point due to a line vortex goes to infinity as the distance approaches zero. This causes the instability of the program and it is especially severe in the case when the vortex wakes are very close to the point of evaluation. It usually happens in the hovering case because the aircraft is stationary and hence the wake left by the blade will interact with the other blade and itself. Fig. 1 and Fig .2 show the spikes appearing in the wake and the aerodynamic forces' graph respectively.

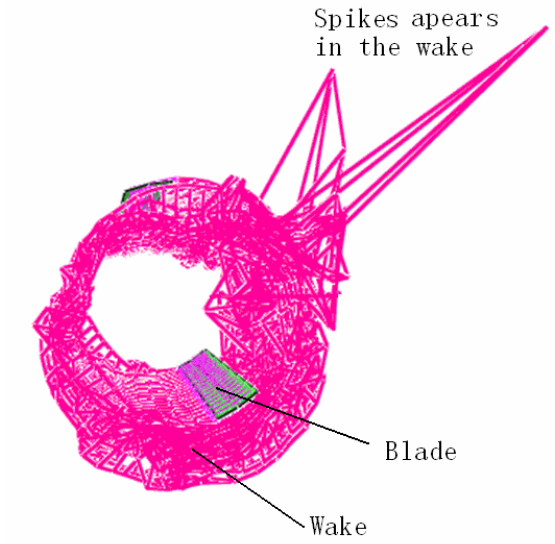

Fig. 1. Spikes appearing during the computation of the wake

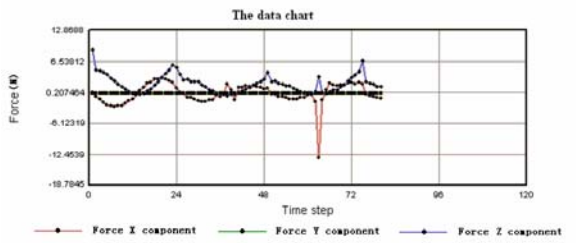

Fig. 2. Forces with spikes showing irregularities

One of the popular methods is to replace the line vortex by a vortex "blob", which is a vortex with an invariable [3] or variable [4] core size. There are different models of the vortex "blob". The common ones include the "Rankine", "Lamb", "Scully" and "Vatistas" models. Fig 3 below shows a comparison of the different models.

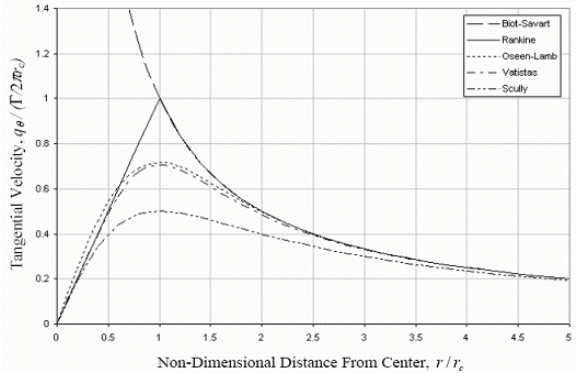

Fig. 3. Comparison of different vortex models

Besides different models, one also has to select the size of the core and the conditions to switch between the original Biot-Savart law and the new model. Since the choice of these 3 variables often depends on specific problems, one has to use some trial and error.

In the first modification, the core size is kept fixed. Results show that the Scully vortex model [5], [6] is the best among the different models.

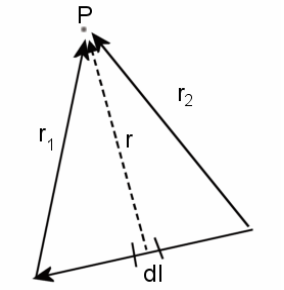

Fig. 4. Induced velocity due to a finite length vortex segment

The velocity induced by the Scully model is given as

$$\Delta\vec{v} = \frac{\Gamma}{4\pi}\vec{r}_1 \times \vec{r}_2 \frac{(r_1 + r_2)(1 - \vec{r}_1 \cdot \vec{r}_2 / r_1 r_2)}{r_1^2 r_2^2 - (\vec{r}_1 \cdot \vec{r}_2)^2 + r_c^2 (r_1^2 + r_2^2 - 2\vec{r}_1 \cdot \vec{r}_2)} \qquad (11)$$

Where r_c is the core radius, Γ is the circulation and r_1 and r_2 are defined in figure 9. When using r_c = 0.2*(length of vortex segment) and induced velocity = 0 when r_1, r_2 and $|r_1 X r_2|^2 < 1X10^{-8}$, the new improved wake model have much less "spikes" than the original program. However, there are still some remaining "spikes" appearing during the visualization of the wake vortex and in the graphs of lift and thrust.

In the second modifications, the vortex core is no longer fixed. Instead, the core is allowed to increase its size, starting from a radius of zero. This model more closely reproduces the actual physical effect. This is because in reality, viscosity will cause the vortex to dissipate and reduce its effect as time progresses. After some time, the effect of the wake vortex will be reduced to zero.

The formula of the core radius r_c is given by

$$r_c(t) = 2.24\sqrt{\upsilon\delta t} \qquad (12)$$

Where υ is the kinematic viscosity of air, t is the time and δ is the turbulent viscosity coefficient. It is given by the expression

$$\delta = 1 + a_1 \frac{\Gamma}{\upsilon} \qquad (13)$$

Where a_1 is the empirical coefficient, which has a nominal value of 10^{-1}, as recommended by [4] . Γ is the circulation at that time step.

As of the first modification, the Scully vortex model gives the best results. Figure 10 and 11 show the results for the fixed and variable core diffusion method respectively. The second modification gives a much smoother graph.

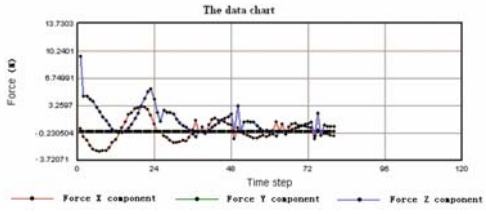

Fig 5. First modification, with fixed core size

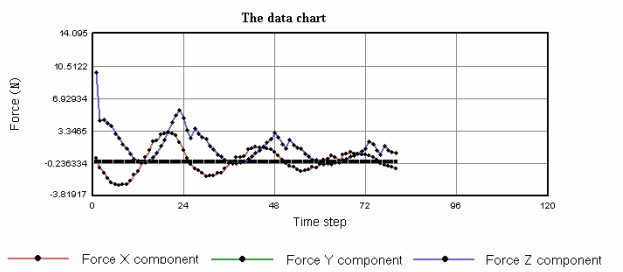

Fig 6. Second modification, with variable core size

3 Results and discussion

A software using UVLM is developed for our Cyclogyro, as shown in figure 7. We also made cycloidal propeller models and a force balance to study the hovering performance of the cycoidal propellers (figure 8). The comparision of the total thrust is shown in figure 9 and figure 10.

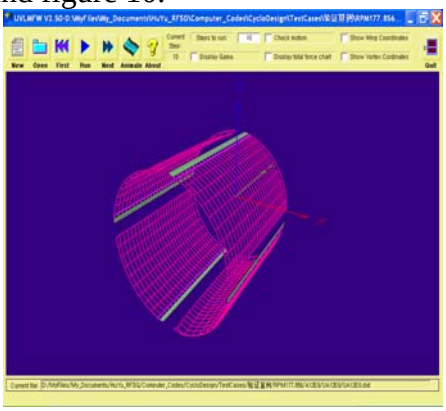

Fig 7. The interface of the software showing the blades and their wake structure

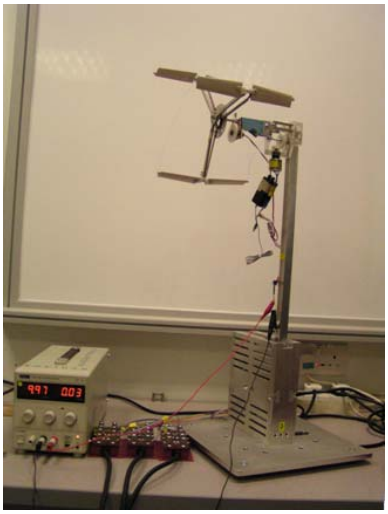

Fig 8. The force balance with the cycloidal propeller test model installed

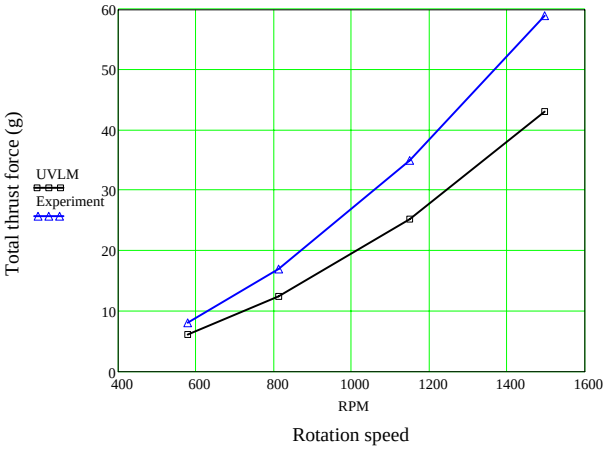

Fig 9. Cycloidal propeller with 70mm radius and NACA 0012 airfoil

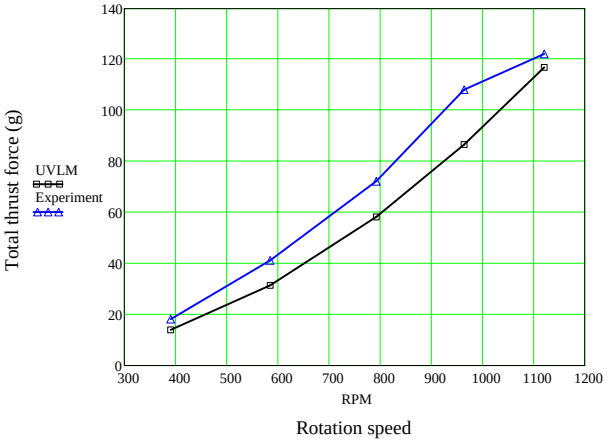

Fig 10. Cycloidal propeller with 150mm radius and flat plate airfoil

The test model is equipped with 3 blades with cord length of 33mm and blade span of 130mm. The Reynolds number for test case in figure 9 is from 8.984×10^{3} to 2.326×10^{4}. The comparison shows that even at such low Reynolds number, simulation based on UVLM with simple viscous correction can obtain acceptable results. These results can be used to evaluate the performance for the engineering purpose.

From the comparison we also find that UVLM tends to under estimate the total lift in both cases of NACA0012 and flat plate airfoil. We think it is because the blade AOA changes very fast and the boundary layer does not act as it used to be in steady state. The viscous correction in our software is based on steady state data and UVLM itself can not simulate the behavior of viscous boundary layer.

As we know, the blades on the cycloidal propeller continuously dive and pull up like an airplane making a loop. When the blade pulls up at the lower cycle, its pitch angle increases rapidly. This kind of motion compresses the boundary layer near the leading edge and delayed the separation [7]. Therefore, even for NACA0012 at such low Reynolds number, the actual trust can be higher than UVLM estimation. For the flat plate blade, the boundary layer will bound to separate at the leading edge and the leading edge vortex is shedding. This produces suction force. The suction force and the pitch up motion can increase the maximum lift coefficient to as high as 3.0, hence further improve the performance [7].

4 Conclusions

The aerodynamics analysis on cycloidal propeller using unsteady vortex lattice method is resented in this paper. A 3-D simulation program, based on the unsteady vortex lattice method has been developed by us. Viscous vortex core models are introduced into the software to deal with the blade wake interaction problem. The results show that the viscous vortex core model can effectively eliminate the error caused by singularity of the vortex rings. The comparison shows that UVLM is able to provide results with good agreement with experiment data. Therefore we can use UVLM for Cyclogyro design.

References

[1] Joseph Katz, Allen Plotkin. *Low Speed Aerodynamics.* Cambridge University Press, 2001

[2] Michel J.S Smith, Peter J. Wilkin, March H. Willianms. The advantages of an unsteady panel method in modeling the aerodynamic forces on rigid flapping wings. *The Journal of Experimental Biology*, 199, pp1073-pp1083, 1996

[3] Christopher J. Szymendera. *Computational free wake analysis of a helicopter rotor*. Masters thesis, The Pennsylvania State University The Graduate School Department of Aerospace Engineering

[4] Tauszig L. A critical evaluation of various approaches for the numerical detection of helicopter blade-vortex interactions. *Journal of the American helicopter society.* pp179-190, July 2000

[5] Scully, M. P., Computation of helicopter rotor wake geometry and its influence on rotor harmonic air loads. *MIT, ASPL-TR-178-1*. March 1975

[6] Zhong Yang. *A hybrid flow analysis for rotors in forward flight.* PhD thesis, Georgia Institute of Technology. 2001

[7] R. W. Prouty, *Helicopter Aerodynamics.* Phillips Publishing, Inc.